

# Surface analysis and optoelectronic studies of Congo thin film

Khitam Abd AL-Adil

**Abstract**—The structural Morphological dependence of the optoelectronic properties of thin films has been studied. The optical constants of the film was studied and the dispersion of the refractive index was discussed in terms of the Wemple Di-Domenico single oscillator model. The real and imaginary part of the dielectric constant of the film was also determined. The volume energy loss increases more than the surface energy loss at their particular peaks. Optically smooth and homogeneous Congo red doped PMMA film was observed for the surface distribution by scan with 20. This film can be used in the form of thin film in dye sensitized solar cells. The self diffraction of Congo red doped PMMA thin film has been studied. The measurement was performed using a low power continuous wave (CW) from solid state laser (SDL) at 473 nm wavelength. The effect of the dye on self diffraction pattern has been investigated.

**Index Terms**- dielectric constant, PMMA film, surface energy loss, self diffraction.

## I. INTRODUCTION

A material is said to be a thin film when it is built up as a thin layer on a substrate by controlled condensation of the individual atomic, molecular or ionic species either directly by a physical process or through a chemical and/or electrochemical reaction. Otherwise, it is a thick film. There are various techniques of producing thin films for scientific application, which include: physical vapour deposition (PVD) technique, chemical vapour deposition (CVD), electrochemical deposition (ECD), hybrid technique, and chemical bath deposition (CBD) technique [1,2]. A thin film has received great attention due to its environmental stability, ease of preparation, and its optical and electrical properties. Much work has been carried out on the molecular design, synthesis, and assembly of structures with desired properties [3-5]. Knowledge of optical constants of a material such as refractive index and extinction coefficient are quite essential to examine material's potential optoelectronic applications [6]. Further, the optical properties may also be closely related to the material's atomic structure, electronic band structure and electrical properties.

In the present work we determine the optical constant and dispersion parameters also the volume energy loss (VELF), surface energy loss (SELF) functions for Congo red thin film. The optical properties of thin films was determined by using transmission and absorbance data spectrum in the wavelength range 0-800 nm. The effect of the dye on self diffraction pattern has been investigated.

## II. MATERIALS AND PREPARATION

Congo red dye, with molecular weight=696.66  $\text{gmol}^{-1}$ , has been selected for our experiments. Congo dye was supplied from Aldrich Company with purity 96%. In our experiment, the host material is Poly (methyl methacrylate) (PMMA) and the ratio of dyes in PMMA by weight is 0.1. The dye-doped PMMA films were prepared as follows: dye and PMMA are dissolved separately in chloroform and then the solution of dye and that of PMMA are mixed, heated (up to 50°C) and stirred for 2 hr, thus the mixed sols of dye and PMMA were obtained. After the sols were filtrated, the films were prepared on a clean glass slide by the repeat-spin-coating method and dried at room temperature (300K) for 48 hr. The film samples have good purity and uniform thickens. The optical absorption spectra are recorded from 0 to 800 nm in steps of 2 nm using Cecil Reflecta-Scan CE -3055 Reflectance Spectrometer at room temperature.

## III. SURFACE ANALYSIS

Characterization of surface topography is important in optical devices. In general, it has been found that diffusion transmission increases with average roughness. Roughness parameters have important applications in linear and nonlinear optics such as linear electro-optical effect, optical filters and optical storage devices. The surface morphology of the thin film is characterized by image processing. It is employed to simulate an optical procedure to measure surface roughness. The three and two dimensional microscopic image surface scan of thin film is displayed in Figs. 1 and 2. As can be seen, two typical morphological features are recognized readily by visual inspection of Figs. 1 and 2. The first is that the granular features of various scales exist in the film and are distributed almost evenly in some ranges. In addition, the granular features possess different irregular shapes, sizes, and separations. No obvious aggregation was observed in the sample. Table.1 shows statistical calculation of film thickness.

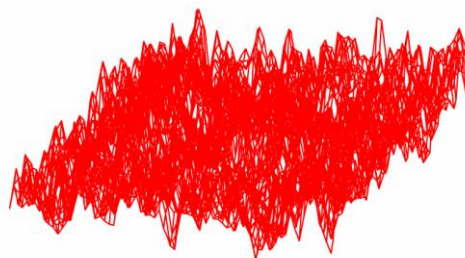


**Fig.1.** 3D microscopic image surface scan of dye film.

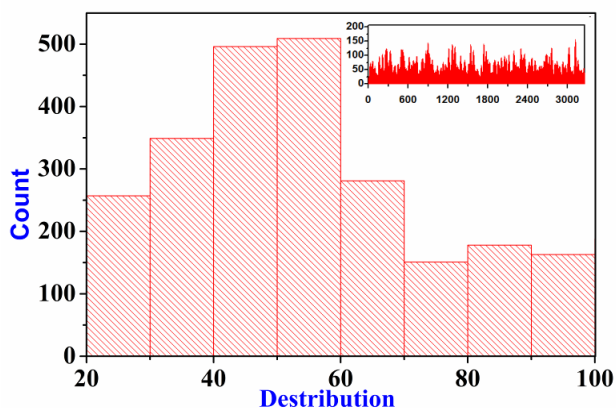


Fig.2. Histogram curve of film surface and microscopic image surface scan of thin film.

Table.1. Statistical value of film thicknesses

Mean	Stander Deviation	Minimum	Median	Maximum
2.40	0.1348	2.056	2.32	3

Fig. 3 shows the plots of  $2\theta$  ( $\theta$  is the angle between the incident beam and the scattering plane, in degrees) versus intensity of the film with Azimuthal angle, Chi, range from 0 to  $360^\circ$ .

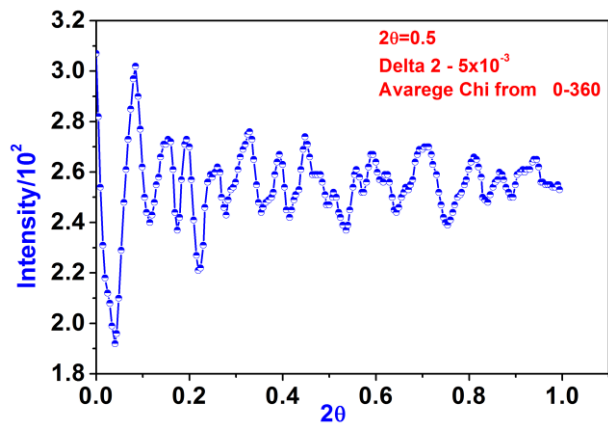


Fig.3 shows the plots of  $2\theta$  with intensity of the film.

#### IV. RESULTS AND DISCUSSIONS

##### A. Optical properties determination

The incoming photons have sufficient energy to excite electrons from the valence band to the conduction band, resulting in strong absorption in sample. The optical absorption edge was determined by the optical absorption, a simple method that provides explanation for the features concerning the band structure of the film. The optical absorption edge was analyzed by the following relationship (Tauc's Procedure) [7].

$$\alpha = \frac{A}{hv} (hv - E_g)^m \quad (1)$$

where,  $\alpha$  is absorption coefficient,  $A$  is an energy-independent constant and  $E_g$  is the optical band gap. The exponent  $m$  depends on the nature of the transition,  $m= 1/2, 2, 3/2$  or  $1/3$  for allowed direct, allowed indirect, forbidden direct or forbidden indirect transitions, respectively. Eq.1 can be written as

$$\frac{d[\ln(\alpha hv)]}{d(hv)} = \frac{m}{hv - E_g} \quad (2)$$

The type of transition can be obtained by determining the value of  $m$ . A discontinuity in the  $d[\ln(\alpha hv)] / d(hv)$  versus  $hv$  plot at the band gap energy, i.e. at  $hv = E_g$  can be observed. The discontinuity at a particular energy value gives the band gap,  $E_g$  [8]. The curves of  $\ln(\alpha hv)$  versus  $\ln(hv - E_g)$  were plotted using the  $E_g$  value to determine  $m$  value and it was found about 2 from the slope of plotted curves. Thus, obtained  $m$  value suggests that the fundamental absorption edge in the films is formed by the indirect allowed transitions. In the transition process, the total energy and momentum of the electron-photon system must be conserved. Fig.4. shows the plots of  $(\alpha hv)^2$  versus  $hv$  of the films. The value of the optical band gap  $E_g$  are given in Table 1.

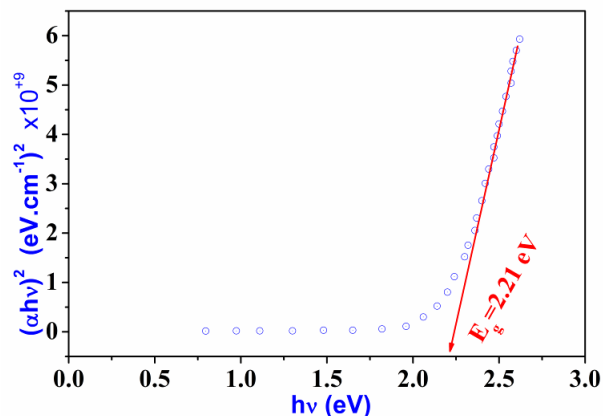


Fig.4.  $(\alpha hv)^2$  vs. photon energy of thin film .

The optical band gap value obtained by this method is suitable for many scientific studies and technological applications, such as gas sensors, and piezoelectric devices.

##### B. Dispersion Characteristics

Measured refractive indices were analyzed by employing the Wemple Di-Domenico single oscillator model [9,10] in the region of normal dispersion ( $\lambda > 400$  nm) and the data were used to obtain the oscillator parameters. Equation 6 describe the relationship between the refractive indices,  $n$ , and the oscillator parameters.

$$\frac{1}{n^2 - 1} = \frac{E_0}{E_d} - \frac{(hv)^2}{E_0 E_d} \quad (3)$$

where,  $hv$  is the photon energy,  $E_0$  is the oscillator energy, and  $E_d$  is the oscillator strength or dispersion energy. Plotting  $(n^2 - 1)^{-1}$  against  $(hv)^2$  allows us to determine the oscillator parameters by fitting a linear function to the lower energy data. The point of intersection with the ordinate at  $hv$

= 0 yield the value of dielectric constant at higher wavelength (static dielectric constant),  $\epsilon_0$ . The values of  $E_0$  and  $E_d$  obtained from the intercept and the slope of the curve and the static refractive index,  $n_0$ , calculated using the relation,  $[n^2(h\nu = 0) = (E_0/E_d) + 1]$ . Fig. 5 shows the plot of  $(n^2 - 1)^{-1}$  against  $(h\nu)^2$ .

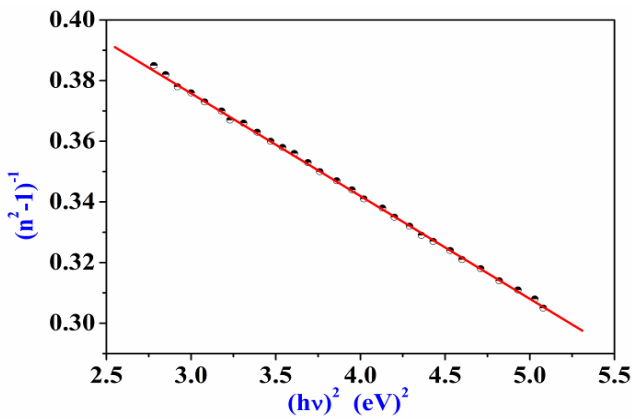


Fig.5 Plot of  $(n^2 - 1)^{-1}$  vs.  $(h\nu)^2$  of thin film.

The oscillator strength parameter,  $F$ , can be calculated using the following relation:

$$F = E_0 E_d \quad (4)$$

The moments of optical dispersion spectra,  $M_{-1}$  and  $M_{-3}$ , can be evaluated using the relations [11]

$$E_0^2 = \frac{M_{-1}}{M_{-3}} \quad (5)$$

$$E_d^2 = \frac{M_{-1}^3}{M_{-3}} \quad (6)$$

Table 2 shows the values of the static refractive index  $n_0$ , the static dielectric constant,  $\epsilon_0$ , oscillator energy,  $E_0$ , dispersion energy,  $E_d$ , the oscillator strength,  $F$ , and the moments of optical dispersion spectra  $M_{-1}, M_{-3}$ .

$E_g$	$E_0$ (eV)	$E_d$ (eV)	$F$ (eV) <sup>2</sup>	$M_{-1}$	$M_{-3}$ (eV) <sup>2</sup>
2.21	3.6	7.4	26.6	2.02	0.15

Table 2. The estimated values of the oscillator parameters of dye film.

It is well-known that polarizability of any solid is proportional to its dielectric constant. The real and imaginary parts of the complex dielectric constant are expressed as [12]:

$$\epsilon_1 = n_2 - k_2 \quad \text{and} \quad \epsilon_2 = 2nk \quad (7)$$

where  $\epsilon_1$  and  $\epsilon_2$  are the real and imaginary parts of the dielectric constant, respectively. The variation of  $\epsilon_1$  and  $\epsilon_2$  values of the thin film with photon energy is shown in Figs. 6 and 7. The real and imaginary parts of dielectric constants

follow the same trend but the values of real part are higher than imaginary part. The variation of the dielectric constant with photon energy indicates that some interactions between photons and electrons in the films are produced in this energy range.

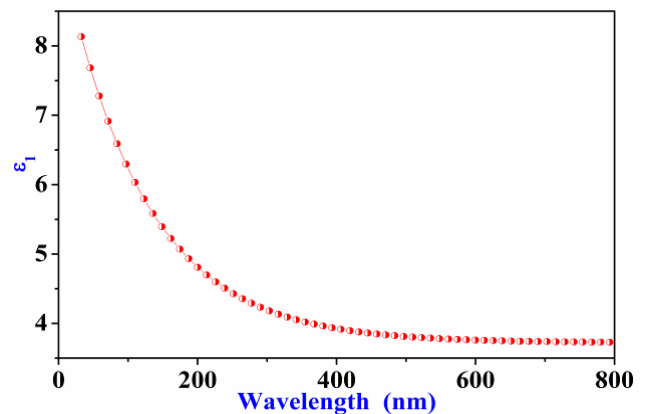


Fig.6. The variation of  $\epsilon_1$  vs.  $h\nu$  of thin film.

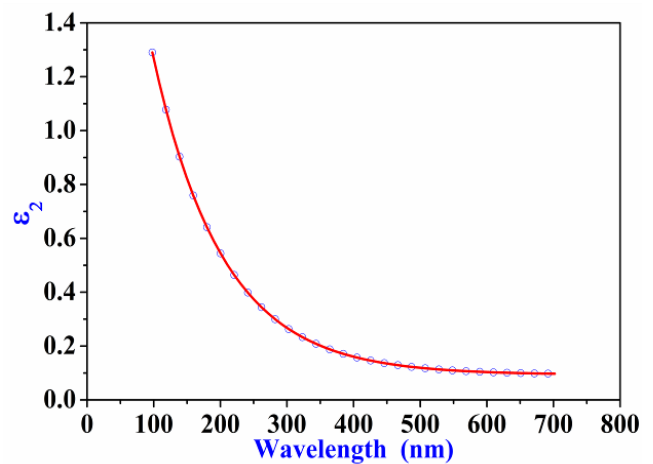


Fig.7. The variation of  $\epsilon_2$  vs.  $h\nu$  of thin film.

#### V. VOLUME ENERGY LOSS AND SURFACE ENERGY LOSS OF THIN FILMS

Quantities of interest in studying the rate of energy loss for electrons passing through a material are the imaginary part of the reciprocal of the dielectric constant, which is known as the volume energy loss (VELF) and the surface energy loss (SELF) functions. They are related to the real and imaginary parts of the dielectric constant by the following relations [13,14] and plotted in Fig.8.

$$SELF = -\text{Im}\left(\frac{1}{1 + \epsilon^*}\right) = \frac{\epsilon_2}{((\epsilon_1 + 1)^2 + \epsilon_2^2)} \quad (8)$$

$$VELF = -\text{Im}\left(\frac{1}{\epsilon^*}\right) = \frac{\epsilon_2}{\epsilon_1^2 + \epsilon_2^2} \quad (9)$$

Figure 8 exhibits volume and surface electron energy loss (VELF and SELF) spectra of the present thin films. It is clear that the energy loss by the free charge carriers when traversing through the bulk material has approximately the same behavior as when they traverse the surface. The two loss features on the surfaces around 4.07 eV. From this figure, there is no significant difference between them at

lower and higher photon energies it is clear that the volume energy loss is greater than surface energy loss at all incident photon energies.

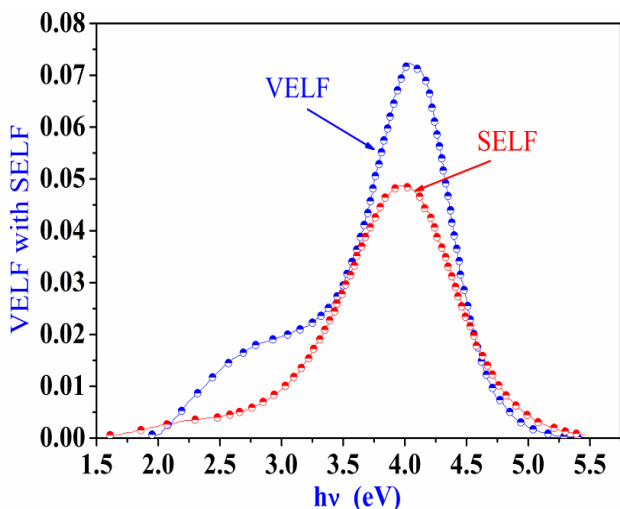


Fig. 8 volume energy loss (VELF) and surface energy loss (SELF) versus photon energy.

#### VI. URBACH'S EMPIRICAL RELATION

Urbach's empirical relation [15] analyzed the absorption which is due to electronic transitions between valence band tail and conduction band states; this kind of absorption is attributed to the phonons assisted indirect electronic transition through the following relation.

$$\alpha = \alpha_0 \exp(h\nu / E_u) \quad (10)$$

where  $\alpha$  is the optical absorption coefficient,  $\alpha_0$  is a constant, and  $E_u$  is the width of the tail (Urbach energy), which characterizes the slope of the exponential edge region. The reciprocal of the slope yields the magnitude of the width of the tail ( $E_u$ ) while the intersection at lower energies gives ( $\alpha_0$ ). The exponential dependence of ( $\alpha$ ) on photon energy for dye film indicates that it obeys Urbach's energy equation. An electronic transition between localized states in the band edge tails is valid in this film.

The exponential dependence of the optical absorption coefficient with photon energy may arise from the electronic transition between the localized state, which tails off in the band gap [16]. The relation of  $\ln\alpha$  versus photon energy is linear for the absorption region near the fundamental absorption edge. This behaviour indicates that the absorption coefficient near the fundamental absorption edge is exponentially dependent on the photon energy and obeys the Urbach rule. Urbach's absorption edge is formed in the region of photon energy below the forbidden band gap. The interaction between lattice vibrations and localized states in tail of the band gap of the dye film has a significant effect on the optical properties of the film [17]. Figure 9 shows the linear dependence of  $\ln\alpha$  on the photon energy and Urbach energy about 181.8meV.

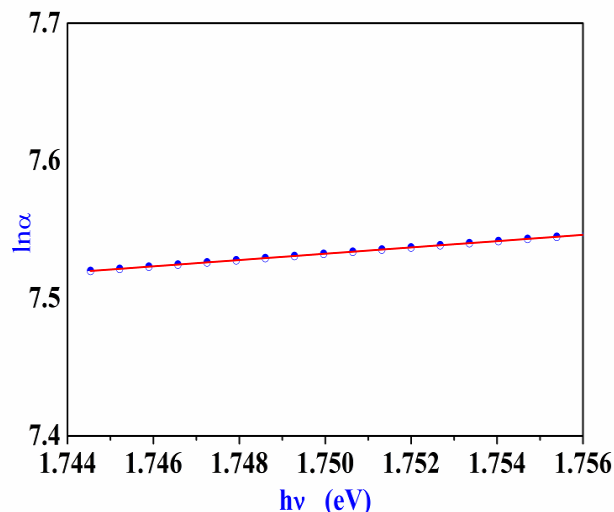


Fig.9.Variation of  $\ln\alpha$  versus  $h\nu$  for thin film.

#### VII. SELF-DIFFRACTION

The self diffraction ring pattern is obtained by keeping the cuvette containing the sample solution at the focal point of the lens. The experimental setup is similar to optical limiting technique [18], the aperture and photo detector are replaced by an observation screen that is centered at the optical axis. As the laser power gradually increases, diffraction rings appear on screen. Images of the beam profile, incident on the sample as well as modified by the nonlinear medium were recorded using a CCD camera placed in the output plane of the sample.

Fig.10 shows the self-diffraction ring pattern formed in the far field using Congo red doped PMMA thin film under CW laser for incident intensity 9.314 kW/cm<sup>2</sup>. This profile demonstrate that a bright diffraction ring gradually becomes thicker from inner to outer side, and the light energy is mainly concentrated inside the outermost ring. Such behaviour corresponds to that observed earlier for divergent Gaussian beams passing through self-defocusing media. Notice that, in general, self-defocusing media have a negative optical nonlinear birefringence  $\Delta n$  [19,20]. The number of rings for the sample is 5.

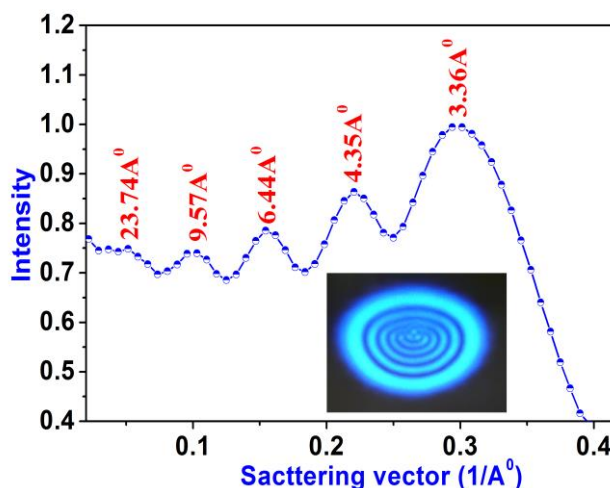


Fig.10. Self-diffraction ring pattern for Congo red doped PMMA thin film



### VIII. CONCLUSION

Optically smooth and homogeneous Congo red doped PMMA film was prepared at room temperature by the spin-coating method. In this work, experimental study has been carried out on the Morphological dependence of the optoelectronic properties of thin film. After preparing, the films were investigated by studying their structural, morphological, and optical properties. The single oscillator Wemple Di-Domenico method was used to calculate their optical constants from the transmittance spectra and the refractive index dispersion of the film. The dispersion of the refractive index in film follows the single electronic oscillator mode relation. The UV-Visible spectroscopic studies showed that, the Congo film have high dielectric constant. Also, Urbach energy has been studied and the energy is about 181.8meV. The self-diffraction ring pattern formed in the far field using Congo red doped PMMA thin film under CW laser for incident intensity  $9.314 \text{ kW/cm}^2$

### REFERENCES

- [1] F.I. Ezema, Turk J. of Phys.5,105 (2005).
- [2] F.I. Ezema, J. of Res. (Sci.), **15**, 343 (2004).
- [3] S. Yin, H. Xu, W. Shi, Y. Gao, Y. Song, J.W.Y. Lam, B. Z. Tang, Polymer **46**, 7670 (2005).
- [4] G. Hallas, A. D. Towns, Dyes Pigments **33**, 319 (1997).
- [5] A. D. Towns, Dyes Pigments **42**, 3 (1999).
- [6] M. Dongol, .Egypt. J. Sol. **25** 33 (2002).
- [7] N.F. Mott, E.A. Davis, *Electronic Process in Non- Crystalline Materials*, Calendron Press, Oxford (1979).
- [8] F. Yakuphanoglu, M. Arslan and S.Z. Yıldız, Opt. Mater. **27**, 1153 (2005).
- [9] S. H. Wemple and M. Di-Domenico, Phys. Rev. Lett. **23**, 1156 (1969).
- [10] S. H. Wemple, and M. Di-Domenico, Phys. Rev. B **3**, 1338 (1971).
- [11] H. Ali Badran, A.Y. Taha, A.F. Abdulkader and C. A.Emshary. J. of Ovonic Research, **8**, 161(2012).
- [12] A.Y.AL-Ahmad, Q. M. A. Hassan, Hussain A. Badran and K. A. Hussain. Optics & Laser Technology **44**,1450 (2012).
- [13] H. Luth. Solid surfaces, interfaces and thin films, 4th edn. (Springer, Berlin, 2010)
- [14] H. Ali Badran, M.F. AL-Mudhaffer, Q. M. A.Hassan and A. Y. AL-Ahmad, Chalcogenide Letters **9**, 483 (2012).
- [15] F. Urbach, Phys. Rev. **92**, 1324 (1953).
- [16] E. Abd EL Wahabb, M.M. El\_Samanoudy, and M. Fadel, Appl. Surf. Sci. **174**, 106 (2001).
- [17] N. F. Mott and E. A. Davis, *Electronic Process in Non\_Crystalline Materials* (Calendron Press, New York, 1979).
- [18] Hussain A. Badran, A. Imran and Q. M. Ali Hassan Optik **127**, 2659 (2016)
- [19] S. D.Durbin, S. M. Arakelian, M. M. Cheung and Y. R. Shen. **C244** (1983) C2161-169.
- [20] A. Y. AL-Ahmad, M. F. AL-Mudhaffer, H. A. Badran and C. A. Emshary, **54**, 72 (2013).



**Khitam Abd Aladil Waheed** was born in 1/5/1979 Missan, Iraq. Got a bachelor from University of Basrah, College of Education in 1998- 2001. On 2010-2013 she got her Master degree in laser physics and nonlinear optical properties from Basrah University, Education College for Pure Sciences, Physics Department. From 2013-Until now she worked as a assistant lecturer in Missan University, Dentistry College, Iraq. Have an experience in Medical physics and Computer Science.